

Multicolour photodetector based on a ZnSe/ZnTe/GaAs heterostructure

S.V. Averin, P.I. Kuznetsov, V.A. Zhitov, L.Yu. Zakharov, V.M. Kotov

Abstract. Structural, optical, and photoelectric properties of a ZnSe/ZnTe/GaAs heterostructure and a metal–semiconductor–metal detector (MSM-detector) based on this heterostructure are investigated. The composition and thickness of individual layers of the heterostructure are determined by the methods of energy dispersive analysis and Raman spectroscopy, and the optical properties are studied using the photoluminescence spectra. The ZnSe/ZnTe/GaAs heterostructure MSM-detector is highly sensitive. In particular, at a wavelength of 620 nm, the detector response signal corresponds to an ampere–watt sensitivity of 0.19 A W^{-1} and an external quantum efficiency of 38%. The MSM-detector photoresponse demonstrates three peaks located at wavelengths of 510, 620, and 870 nm. For the MSM-diode with a pin contact width of $2.8 \text{ }\mu\text{m}$, distances between them of $2.8 \text{ }\mu\text{m}$, and a total photosensitive area of $100 \times 100 \text{ }\mu\text{m}^2$, the dark current density at room temperature constitutes $10^{-8} \text{ A cm}^{-2}$.

Keywords: photodetector, MSM-diode, heterostructure, dark current, spectral response.

1. Introduction

One of the promising areas of research in the field of photoelectric converters is the development of band detectors for individual areas of UV, visible and near-IR spectral regions [1]. Such multicolour photodetectors are required for a number of practical applications, including military science, spectroscopy, imaging, environmental monitoring, communication systems, etc. [2]. In these spectral regions, silicon and gallium arsenide photodetectors are commonly used. However, they perform signal detection in a fairly wide range of wavelengths and do not possess spectral selectivity. To ensure selective response at certain wavelengths, such detectors require the use of external filters, which leads to a complication of the receiving system and significantly reduces its sensitivity. Selective detection of two or more separately located portions of the radiation spectrum makes it possible to significantly facilitate the analysis of the observed object, since in this case it is possible to determine its emissivity as a function of the wavelength and to implement the possibility of selective isolation and recognition [3].

S.V. Averin, P.I. Kuznetsov, V.A. Zhitov, L.Yu. Zakharov, V.M. Kotov
V.A. Kotelnikov Institute of Radio Engineering and Electronics (Fryazino Branch), Russian Academy of Sciences, pl. Akad. Vvedenskogo 1, 141190 Fryazino, Moscow region, Russia;
e-mail: sva278@ire216.msk.su

Received 27 November 2017
Kvantovaya Elektronika 48 (7) 675–678 (2018)
Translated by M.A. Monastyrskiy

The key moment in the development of efficient selectively sensitive detectors in these spectral regions is the manufacture of nanoheterostructures of wide bandgap semiconductor compounds. We have recently investigated the detection properties of low-dimensional heterostructures with ZnCdS quantum wells separated by ZnMgS barrier layers, which provide two-colour UV detection at wavelengths of 350 and 450 nm [4].

This paper presents the results of experimental studies on the structural, optical, and electrical characteristics of the ZnSe/ZnTe/GaAs heterostructure and the metal–semiconductor–metal photodiode (MSM-photodiode) based on that structure. The MSM-detector has high sensitivity. At a wavelength of 620 nm, the detector response signal corresponds to an ampere–watt sensitivity of $S = 0.19 \text{ A W}^{-1}$ and an external quantum efficiency of $\text{EQE} = 38\%$. Spectral characteristic of the MSM-detector provides detection of three separately located wavelengths of visible and IR radiation by a single photodiode.

2. Experimental results

The heterostructure was grown using the MOCVD method with successive deposition of twelve pairs of ZnSe/ZnTe layers onto a semi-insulating substrate of GaAs (Fig. 1). A thin coating layer of ZnSe was grown on atop the structure. The deposition process was performed in hydrogen atmosphere at a temperature of 470°C using diethylzinc, diethylselenide, and diethyltelluride as initial reagents. With the growth of the ZnSe and ZnTe layers, a double excess of chalcogen in the gas phase was maintained. Before the growth of each new layer, a

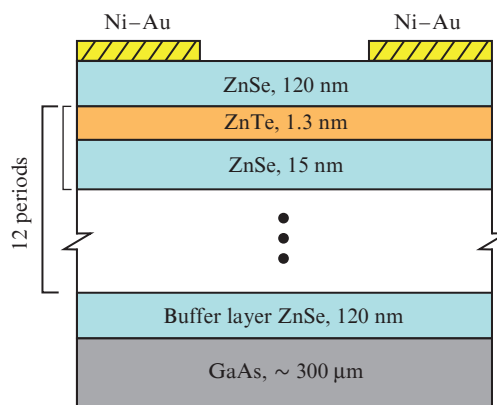


Figure 1. System of layers of the ZnSe/ZnTe/GaAs heterostructure and pin contacts of the MSM-diode on its basis.

pause of 10 seconds was made. The quality of the surface growth was assessed using a SmartSPM scanning probe microscope (AIST-NT). The heterostructure surface was quite dense and consisted of uniformly distributed small grains (Fig. 2). According to the measurements, the growth surface roughness was 3.2 nm over an area of $2 \times 2 \mu\text{m}$.

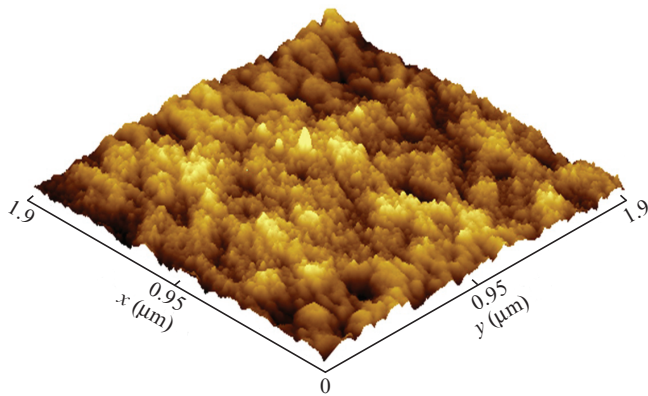


Figure 2. Microphotograph of the ZnSe/ZnTe/GaAs structure surface.

2.1. Method of energy dispersive analysis (EDS)

An X-MaxN energy dispersive spectrometer (Oxford Instruments) with the crystal's active zone area of 50 mm^2 was used for qualitative and quantitative determination of the heterostructure composition. The results were processed in the INCA program (Oxford Instruments, version 21). To standardise and optimise the profiles of the emission lines of characteristic radiation, simple reference substances were used: crystalline Bi_2Se_3 (for SeL_α line standardisation), ZnS (ZnL_α line), and PbTe (TeL_α line). The measurements of reference substances and analysis of samples were performed under identical conditions at an accelerating voltage of 10 kV, an electron probe current of 1.4 nA, and a time constant of 5 ms. The rate of data accumulation was 12×10^3 pulses per second at the 'dead time' of 25% to 30%. The time of spectra accumulation in the energy range from 0 to 10 keV with dispersion over 2048 channels was set equal to 100 s. Under these conditions, the dispersion of component concentrations to be determined did not exceed 0.5%, and the detection threshold for all the analysed elements was 0.03–0.05 mass %. Figure 3

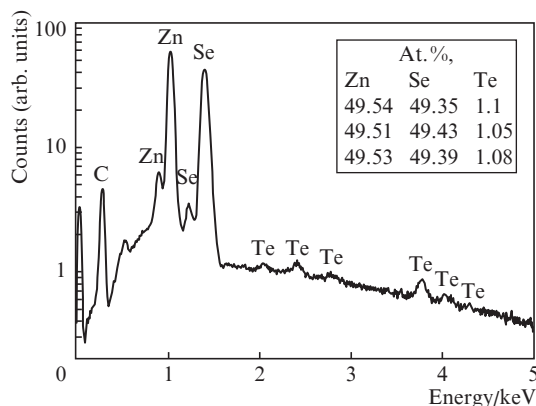


Figure 3. EDS spectrum of the ZnSe/ZnTe heterostructure.

shows the EDS spectrum of the initial ZnSe/ZnTe heterostructure. Three sample points were analysed, in which the tellurium content was varied within the range of 1.05–1.1 at.%. The calculation showed that the total thickness of 12 ZnTe layers was 9.5 nm; hence, the single layer thickness was 0.8 nm. This is 1.6 times less than the thickness calculated from the kinetics of the epitaxial deposition process, and seems to be due to the deposition process nonstationarity in a short time interval of growth of a single ZnTe layer (5.5 s).

2.2. Raman scattering

Raman scattering spectra were measured with a XPlora spectrometer (Horiba Scientific) using a 532 nm wavelength laser and a $100\times$ objective that focuses laser radiation into a spot of $\sim 1 \mu\text{m}$ in diameter. For the measurement, a $1800 \text{ lines mm}^{-1}$ grating was used, the accumulation time was $3 \times 30 \text{ s}$, the laser power was above 3 mW, and the spectra recording range was from 50 to 1000 cm^{-1} . Figure 4 [curve (3)] shows the Raman spectrum of the heterostructure that serves as a basis for subsequent manufacture of an MSM-detector, on which the ZnSe LO-mode and the corresponding weak modes of ZnTe and GaAs substrates are visible. For comparison, the same Figure shows the spectra of epitaxial ZnSe and ZnTe films of equal thickness grown on semi-insulating (100) GaAs substrates [curves (1) and (2)]. Comparison of these curves with curve (3) makes it possible to identify Raman scattering peaks for the investigated heterostructure at frequencies of 200 (ZnTe), 248 (ZnSe), and 289 (GaAs) cm^{-1} .

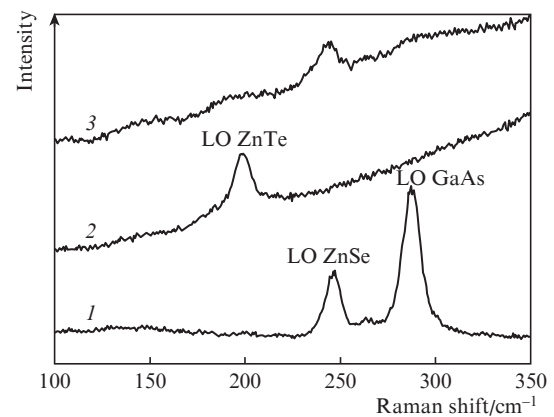


Figure 4. Raman scattering spectra of the ZnSe/ZnTe heterostructure under investigation (3) and the ZnTe and ZnSe epitaxial films with a thickness of 400 nm on the GaAs semi-insulating substrate (1, 2).

2.3. Photoluminescence

The photoluminescence signal spectra were measured at room temperature. As excitation sources, a pulsed N_2 laser with a wavelength of 337 nm and a continuous He–Cd laser with a wavelength of 441.6 nm were used. The radiation from the He–Cd laser was focused into a spot of $30 \mu\text{m}$ in diameter, while the radiation from the N_2 laser was focused into a spot of $50 \mu\text{m}$ in diameter. The optical excitation signal density was varied with the use of neutral filters.

The photoluminescence signal spectra of the ZnSe/ZnTe heterostructure under investigation are presented in Fig. 5. When the sample is excited with the He–Cd laser radiation, only indirect transitions with a maximum at $\sim 640 \text{ nm}$ are

observed, the position of which does not depend on the optical excitation signal density (Fig. 5a). When the sample is excited by a pulsed N₂ laser, the maxima of the photoluminescence spectra are shifted toward shorter wavelengths (600 nm region); with an increase in the optical excitation signal density, the spectral region is shifted to shorter wavelengths due to the indirect transition, and an amplification of the direct band transition signal in the ZnSe layers is observed (Fig. 5b). The short-wavelength shift of the photoluminescence signal recorded with increasing optical excitation signal density confirms the presence of a type-II transition in the ZnSe/ZnTe superlattice under study [5].

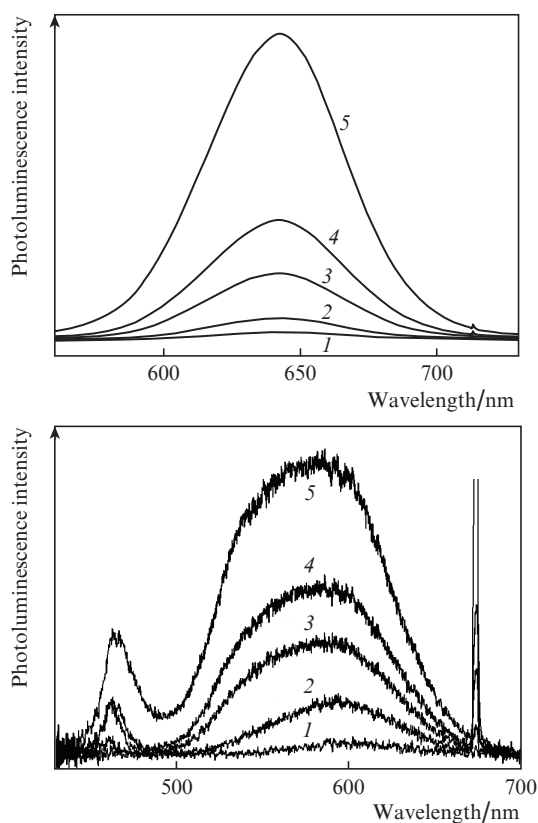


Figure 5. Spectra of a photoluminescence signal excited (a) by the radiation from a continuous He–Cd laser ($\lambda_{\text{ex}} = 441.6$ nm) at an optical excitation density of (1) 9, (2) 18, (3) 36, (4) 50 and (5) 100 W cm^{-2} and (b) by the radiation from a pulsed N₂ laser ($\lambda_{\text{ex}} = 337$ nm) at an excitation density of (1) 10^6 , (2) 5×10^6 , (3) 2.1×10^7 , (4) 3.7×10^7 and (5) 10^8 W cm^{-2} . $T = 300 \text{ K}$.

2.4. MSM-diode characteristics

On the heterostructure grown by photolithography methods, the MSM-diode pin contacts with a width of $2.8 \mu\text{m}$, a distance between them of $2.8 \mu\text{m}$, and a total area of the detector photosensitive region of $100 \times 100 \mu\text{m}$ were formed. The Ni–Au pair was used as a Schottky contact metal. Figure 6 shows a microphotograph of the ZnSe/ZnTe heterostructure surface and the Schottky contact system of the MSM-diode.

The volt–ampere characteristics of the manufactured MSM-detectors were investigated with an Agilent B 1500A semiconductor device analyser. X-ray examination has shown that in the case of thin (less than 1 nm) epitaxial ZnTe layers, the heterostructure is isomorphous and does not have many

structural defects. As a result, the MSM-detector based on the ZnSe/ZnTe superlattice has low dark currents even at high bias voltages. The dark current constituted 10^{-12} A at a bias voltage of 40 V, which is more than two orders of magnitude less than that of AlGaIn-based MSM-detectors with almost the same geometry of contacts [6], and is comparable with dark currents of the low-dimensional ZnCdS/ZnMgS/GaP structure [4]. The dark current density of the MSM-detector based on the ZnSe/ZnTe/GaAs heterostructure at room temperature constituted $10^{-8} \text{ A cm}^{-2}$.

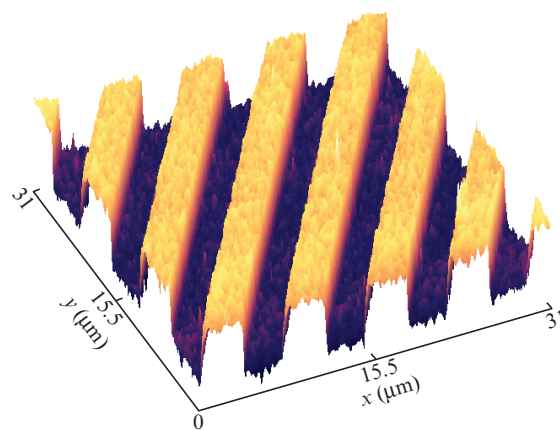


Figure 6. ZnSe/ZnTe/GaAs heterostructure surface and pin contacts of the MSM-photodiode.

2.5. Spectral photosensitivity

Measurements of spectral photosensitivity of the diode structures in question were performed at room temperature using a xenon lamp as a radiation source, a monochromator, a modulator, and a selective voltmeter in the regime of synchronous detection of the electric signal in the MSM-diode being investigated. The power of optical radiation incident on this photodiode was measured by a calibrated silicon photodiode. The ampere–watt sensitivity of the photodetector was determined as a ratio of the measured signal current in the MSM-diode to the radiation power of a xenon lamp at the corresponding wavelength.

Figure 7 demonstrates the photoresponse signal of the MSM-detector based on the ZnSe/ZnTe/GaAs heterostructure as a function of the optical radiation wavelength. The detector photoresponse shows three peaks located at wavelengths of 510, 620, and 870 nm. The position of the detector response signal maximum at a wavelength of 620 nm virtually coincides with the photoluminescence signal maximum of the ZnSe/ZnTe superlattice (see Fig. 5a). The peak of the detector response signal at a wavelength of 510 nm is stipulated by the interference of light between the upper and lower boundaries of the semiconductor structure, and can be adjusted by an appropriate change in the thicknesses of the heterostructure layers (a similar effect was observed in paper [7] with the interference of light in the ZnSSeTe/GaAs epitaxial layers). An increase in the bias voltage from 20 to 60 V makes it possible to exclude the blocking effect of the heterobarrier at the ZnSe/GaAs interface; hence, the detector ensures efficient collection of photocarriers from the underlying GaAs layer [curve (5) in Fig. 7]. This explains the presence of a peak in the detector photoresponse signal at a wavelength of 870 nm

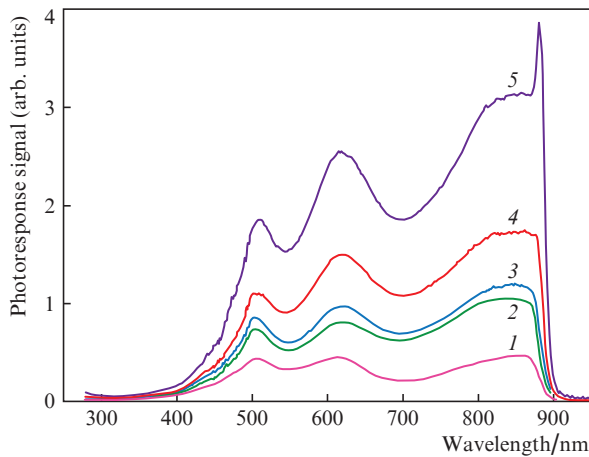


Figure 7. Photoresponse signal spectra of the MSM-detector based on the ZnSe/ZnTe/GaAs heterostructure at a bias voltages of (1) 20, (2) 30, (3) 40, (4) 50 and (5) 60 V.

(GaAs absorption band edge) at a bias voltage of 60 V. Thus, the spectral characteristic of the detector demonstrates the possibility of selective detection of visible and IR radiation in the wavelength range of 500–870 nm.

The detector has a high sensitivity. At a wavelength of 620 nm, the detector response signal corresponds to the ampere–watt sensitivity $S = 0.19 \text{ A W}^{-1}$ and the external quantum efficiency $\text{EQE} = 38\%$, and at a wavelength of 840 nm $S = 0.28 \text{ A W}^{-1}$ and $\text{EQE} = 41\%$. If the light losses due to reflection from the pin contacts and semiconductor surface are taken into account, the detector quantum efficiency at the corresponding wavelengths is close to the calculated one. For comparison, the external quantum efficiency of the GaAs-based MSM-diode with the use of surface plasmons constitutes 46% at a resonance wavelength of 790 nm [8]. The internal quantum efficiency of the ZnSTeSe/ZnSe/GaAs photodiode is 42% at a wavelength of 620 nm and 75% at a wavelength of 820 nm [7]. A SWIR-detector with the n–i–p structure on the InAs/InAs_{1-x}Sb_x/AlAs_{1-x}Sb_x type-II superlattice exhibits an ampere–watt sensitivity $S = 0.47 \text{ A W}^{-1}$ and an efficiency $\text{EQE} = 37\%$ at a wavelength of 1.5 μm , but at a significantly higher dark current density of $9.6 \times 10^{-5} \text{ A cm}^{-2}$ [9]. The quantum efficiency of a pin detector based on the InAs/GaAsSb superlattice is 18.6% at a wavelength of 1.15 μm , an ampere–watt sensitivity is $S = 0.17 \text{ A W}^{-1}$, with the dark current density constituting $2.9 \times 10^{-9} \text{ A cm}^{-2}$ at 77 K [10]. It should be noted that the photoresponse spectrum of the MSM-detector we have proposed also has a weak burst at a wavelength of 470 nm due to the presence of the ZnSe cover layer. The low efficiency at this wavelength is caused by strong surface recombination.

3. Conclusions

We have studied structural, electrical, and optical properties of the ZnSe/ZnTe/GaAs heterostructure. The composition and thickness of individual layers of the heterostructure are determined by the methods of energy dispersive analysis and Raman spectroscopy, and the optical properties are studied using photoluminescence spectra. A short-wavelength shift in the photoluminescence signal, observed with increasing optical excitation density, confirms the presence of a type-II transition in the ZnSe/ZnTe superlattice. On the basis of the

ZnSe/ZnTe/GaAs heterostructure, a MSM-photodetector was manufactured and investigated. The detector exhibits low dark current, high ampere–watt sensitivity and quantum efficiency. The maximum signal of the MSM-detector photoresponse at a wavelength of 620 nm corresponds to a current sensitivity of 0.19 A W^{-1} and an external quantum efficiency of 38%. For the MSM-heterophotodiode with a width of pin contacts of 2.8 μm , a distance between them of 2.8 μm , and a total photosensitive area of $100 \times 100 \mu\text{m}^2$, the dark current density at room temperature was $10^{-8} \text{ A cm}^{-2}$. The detector spectral characteristic demonstrates the possibility of selective detection of visible and IR radiation in the wavelength range from 500 to 870 nm.

Acknowledgements. The authors are grateful to V.D. Shcherbakov, V.O. Yapaskurt, and M.P. Temiryazeva for their assistance in conducting experiments on Raman spectroscopy, energy dispersive analysis, and atomic force microscopy of the samples.

The work was partially supported by the Russian Foundation for Basic Research (Project No. 17-07-00205).

References

- Blank T.V., Gol'dberg Yu.A. *Fiz. Tekh. Poluprovodn.*, **37**, 1025 (2003).
- Steenbergen E.H., DiNezza M.J., Dettlaff W.H.G., Lim S.H., Zhang Y.-H. *Appl. Phys. Lett.*, **97**, 161111-1 (2010).
- Rogalski A. *Acta Physica Polonica A*, **116**, 389 (2009).
- Averin S.V., Kuznetsov P.I., Zhitov V.A., Zakharov L.Yu., Kotov V.M., Alkeev N.V. *Sol. State Electron.*, **114**, 135 (2015).
- Ledentsov N.N., Bohler J., Beer M., Heinrichsdorff F., Grundmann M., Bimberg D., Ivanov S.V., Meltser B.Ya., Shaposhnikov S.V., Yassievich I.N., Faleev N.N., Kop'ev P.S., Alferov Zh.I. *Phys. Rev. B*, **52**, 14058 (1995).
- Averin S.V., Kuznetsov P.I., Zhitov V.A., Alkeev N.V. *Sol. State Electron.*, **52**, 618 (2008).
- Chen W.R., Meen T.H., Cheng Y.C., Lin W.J. *IEEE Electron. Device Lett.*, **27**, 347 (2006).
- Collin St., Pardo F., Averin S.V., Bardou N., Pelouard J.-L. *Quantum Electron.*, **40**, 421 (2010) [*Kvantovaya Elektron.*, **40**, 421 (2010)].
- Haddadi A., Suo X.V., Adhikary S., Dianat P., Hoang A.M., Razeghi M. *Appl. Phys. Lett.*, **107**, 141104-1 (2015).
- Zhang Y., Ma W., Huang J., Cao Y., Liu K., Huang W., Zhao Ch., Ji H., Yang T. *IEEE Electron Device Lett.*, **37**, 1166 (2016).